# Localization and Role of Manganese Superoxide Dismutase in a Marine Diatom[1][OA]

**Felisa Wolfe-Simon[2]*, Valentin Starovoytov, John R. Reinfelder, Oscar Schofield, and Paul G. Falkowski**

Environmental Biophysics and Molecular Ecology Program, Institute of Marine and Coastal Sciences (F.W.-S., O.S., P.G.F.), and Department of Environmental Science (J.R.R.), Rutgers University, New Brunswick, New Jersey 08901; and Department of Cell Biology and Neuroscience (V.S.), and Department of Geological Science, Wright Geological Laboratory (P.G.F.), Rutgers University, Piscataway, New Jersey 08854

Superoxide dismutase (SOD) catalyzes the transformation of superoxide to molecular oxygen and hydrogen peroxide. Of the four known SOD isoforms, distinguished by their metal cofactor (iron, manganese [Mn], copper/zinc, nickel), MnSOD is the dominant form in the diatom *Thalassiosira pseudonana*. We cloned the MnSOD gene, *sod*A, using the expression vector pBAD, overexpressed the product in *Escherichia coli*, and purified the mature protein (TpMnSOD). This recombinant enzyme was used to generate a polyclonal antibody in rabbit that recognizes MnSOD in *T. pseudonana*. Based on quantitative immunoblots, we calculate that in vivo concentrations of TpMnSOD are approximately 0.9 amol cell$^{-1}$ using the recombinant protein as a standard. Immunogold staining indicates that TpMnSOD is localized in the chloroplasts, which is in contrast to most other eukaryotic algae (including chlorophytes and embryophytes) where MnSOD is localized exclusively in mitochondria. Based on the photosynthetic Mn complex in photosystem II, cellular Mn budgets cannot account for 50% to 80% of measured Mn within diatom cells. Our results reveal that chloroplastic MnSOD accounts for 10% to 20% of cellular Mn, depending on incident light intensity and cellular growth rate. Indeed, our analysis indicates that TpMnSOD accounts for 1.4% (±0.2%) of the total protein in the cell. The TpMnSOD has a rapid turnover rate with an apparent half-life of 6 to 8 h when grown under continuous light. TpMnSOD concentrations increase relative to chlorophyll, with an increase in incident light intensity to minimize photosynthetic oxidative stress. The employment of a Mn-based SOD, linked to photosynthetic stress in *T. pseudonana*, may contribute to the continued success of diatoms in the low iron regions of the modern ocean.

All aerobic organisms produce intracellular and extracellular reactive oxygen species (ROS) as metabolic byproducts (Haliwell, 1982; Asada, 1999; Apel and Hirt, 2004). Photoautotrophs also produce ROS through photosynthesis (Falkowski and Raven, 1997; Anderson et al., 1999; Wolfe-Simon et al., 2005). The ROS byproducts include superoxide ($O_2^{\cdot-}$), hydrogen peroxide, and hydroxyl radical (Haliwell, 1982). In addition to being highly reactive, $O_2^{\cdot-}$ is particularly destructive because it cannot diffuse across cell membranes and, therefore, must be destroyed at the site of production. Superoxide dismutases (SODs) are a polyphyletic family of enzymes that protect cells from $O_2^{\cdot-}$. SODs come in four isoforms, recognized by their metal center cofactors (iron [Fe], manganese [Mn], copper [Cu]/zinc [Zn], and nickel [Ni]), and catalyze the destruction of $O_2^{\cdot-}$ to hydrogen peroxide and $O_2$. This key antioxidant has been well studied in many eukaryotic systems, including metazoa and plants (Bowler et al., 1992; Scandalios, 1993; Fridovich, 1995; Raychaudhuri and Deng, 2000; Zelko et al., 2002). However, few studies on the intracellular regulation of SOD in diatoms are available, which is unfortunate, as these algae dominate the flux of carbon in the contemporary ocean (Falkowski et al., 2004b).

Diatoms appear to rely primarily on the Mn form of SOD (MnSOD; Peers and Price, 2004); therefore, understanding the regulation of MnSOD in diatoms is important, as this enzyme must be critical to the cells' ability to cope with oxidative stress. The regulation and subcellular localization of MnSOD varies significantly among algal taxa (Wolfe-Simon et al., 2005). In cyanobacteria, MnSOD is found in the periplasm and is associated with the thylakoid membranes (Herbert et al., 1992; Chen et al., 2001; Li et al., 2002). In contrast, MnSOD is found in the mitochondria of embryophytes, chlorophytes, and dinoflagellates (Kliebenstein et al., 1998; Kitayama et al., 1999; Wu et al., 1999; Okamoto et al., 2001; Okomoto et al., 2001; Fink and Scandalios, 2002). Although some information has been shown regarding SOD in diatoms (Huang et al., 2005; Ken et al., 2005), no information on the subcellular localization of MnSOD and the associated kinetics in diatoms is available.

[1] This work was supported by the National Science Foundation (grant no. OCE 0084032, Biocomplexity: The Evolution and Radiation of Eukaryotic Phytoplankton Taxa, to P.G.F. and O.S.) and by Rutgers University (Excellence Fellowship to F.W.-S.).

[2] Present address: Metallomics Laboratory, Department of Chemistry and Biochemistry, Arizona State University, Tempe, AZ 85287.

* Corresponding author; e-mail fwolfe@asu.edu; fax 480–965–2747.

The author responsible for distribution of materials integral to the findings presented in this article in accordance with the policy described in the Instructions for Authors (www.plantphysiol.org) is: Paul G. Falkowski (falko@imcs.rutgers.edu).

[OA] Open Access articles can be viewed online without a subscription.

www.plantphysiol.org/cgi/doi/10.1104/pp.106.088963

Given our lack of understanding of MnSOD in diatoms, despite their global significance, we examined the expression and preliminary regulation of MnSOD in the bloom-forming diatom *Thalassiosira pseudonana* CCMP1335 (Ziemann et al., 1991; Levasseur et al., 1992; Zigone et al., 1995; Cabecadas et al., 1999). Our results indicate that MnSOD is localized in the chloroplast and has a rapid turnover rate mediated by incident light levels that are closely coupled to photosynthetic activity.

## RESULTS

### Native Molecular Mass and Western Analyses

Western blots from denaturing PAGE of crude cell extracts (Fig. 1) probed with anti-TPMnSOD reveal a major band of approximately 23 kD, which corresponds well with the predicted subunit molecular mass of 22.8 kD for MnSOD based on sequence analysis. The anti-TpMnSOD cross reacted with other diatom species and weakly recognized MnSOD in several dinoflagellates (Table I). Interestingly, there was no anti-TpMnSOD cross reactivity with two other heterokonts: *Nannochloropsis oculata* and *Heterosigma akashiwo*. No reactivity was observed in the chlorophytes, cyanobacteria, prymnesiophytes, cryptophytes, and rhodophytes.

### MnSOD and the Cellular Mn Budget in Diatoms

Based on quantitative immunoanalyses of MnSOD in nutrient-replete, exponentially growing cultures of *T. pseudonana*, this marine diatom maintains 0.91 amol MnSOD per cell when grown at moderate light levels. This quantity of MnSOD accounts for 1.4% (±0.2%) of the total cellular protein (Table II). This pool turns over rapidly; TpMnSOD is virtually undetectable after 16 h under continuous light when protein synthesis is blocked (Fig. 2), corresponding to a 5- to 8-h half-life. The turnover was mediated by light as the protein was detectable even after 27 h when cells were kept in darkness, regardless of whether protein synthesis was inhibited.

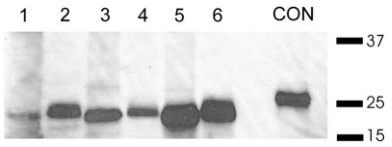


**Figure 1.** Immunoblot of selected diatom species. Immunoblots showing the anti-TpMnSOD antibody we produced cross reacted with multiple diatom species. The phylum specificity of this antibody suggests that all diatoms have a MnSOD with similar structure. All lanes loaded with 30 $\mu$g total protein (except control loaded with 10 ng pure recombinant TpMnSOD): lane 1, *Ditylum brightwellii* CCMP358; lane 2, *Navicula incerta* CCMP542; lane 3, *Nitzschia brevirostris* CCMP551; lane 4, *Stephanopyxis turris* CCMP815; lane 5, *T. pseudonana* CCMP1010; lane 6, *Skeletonema costatum* CCMP1332; CON, control protein overexpressed and purified recombinant TpMnSOD. Note: *T. pseudonana* strain used in this immunoblot is CCMP1010 and different than CCMP1335, which is the one used for cloning and overexpression of *sod*A. Marker indicates molecular mass standards in kilodaltons.

**Table I.** *Antibody cross reactivity*

We reverse transcribed, amplified, and cloned the gene for MnSOD from freshly extracted *T. pseudonana* mRNA. We then raised an antibody in rabbits to the recombinant protein and tested the antibody against a wide range of whole cell protein extractions from cyanobacteria, primary green, primary red, and secondary red algae. Here, we present data showing the specificity of this antibody. It primarily recognizes only diatoms and only weakly some dinoflagellates. It did not cross react with any other phylum or class of algae. All algae were grown in pure culture at optimal conditions as recommended by the Culture Collection of Marine Phytoplankton (CCMP; www.bigelow.org). +, Positive recognition; ~, weak recognition; −, no recognition.

| Taxa Identification | CCMP | Recognition |
|---|---|---|
| Bacillaryophyta | | |
| *Ditylum brightwellii* | 358 | + |
| *Navicula incerta* | 542 | + |
| *Nitzschia brevirostris* | 551 | + |
| *Stephanopyxis turris* | 815 | + |
| *Thalassiosira pseudonana* | 1010 | + |
| *Skeletonema costatum* | 1332 | + |
| Dinophyceae | | |
| *Karlodinium micrum* | 415 | ~ |
| *Heterocapsa triquetra* | 449 | ~ |
| *Amphidinium carterae* | 1314 | ~ |
| *Prorocentrum minimum* | 1329 | ~ |
| Eustigmatophyceae | | |
| *Nannochloropsis oculata* | 525 | − |
| Raphidophyceae | | |
| *Heterosigma akashiwo* | 1680 | − |
| Chlorophyta | | |
| *Dunaliella tertiolecta* | 1320 | − |
| *Pyramimonas parkeae* | 724 | − |
| *Nannochloris atomus* | 509 | − |
| *Pycnococcus provasolii* | 1203 | − |
| *Tetraselmis marina* | 898 | − |
| Prymnesiophyta | | |
| *Isochrysis galbana* | 1323 | − |
| *Emiliania huxleyi* | 373 | − |
| Cryptophyceae | | |
| *Rhodomonas salina* | 1319 | − |
| Rhodophyta | | |
| *Porphyridium* sp. | – | − |
| Cyanobacteria | | |
| *Trichodesmium* sp. IMS101 | – | − |
| *Synechocystis* sp. PCC6803 | – | − |

The total Mn associated with TpMnSOD ranges between 10% and 20% of the total cellular Mn (Fig. 3; see legend for calculation details). Raven (1990) estimated that between 2 and 4 $\mu$mol Mn mol $C^{-1}$ are needed to support the Mn requirement of the PSII Mn complex in *T. pseudonana*, which would account for approximately 60% of total Mn within a cell (Sunda and Huntsman, 1986, 1998; Raven, 1990). Based on immunoquantitative analyses, MnSOD accounts for another 18% of the Mn budget. Thus, approximately 80% of the total Mn budget is associated with MnSOD and PSII.

**Table II.** *Statistics for MnSOD in T. pseudonana CCMP1335*

These data show the cell-specific MnSOD budget based on quantitative immunoanalyses (see "Materials and Methods"). Although MnSOD accounts for a small percentage of the total protein, it is an important pool of Mn in the cell. Cells were grown under continuous light, 120 $\mu$mol $m^{-2}$ $s^{-1}$ at 20°C.

| Unit of Measure | Valuation |
|---|---|
| Protein mass per cell | 19.8 ± 3 fg MnSOD $cell^{-1}$ |
| Molecules per cell | 5.5 ± 0.9 × $10^5$ MnSOD $cell^{-1}$[a] |
| Molecules per cell | 2.7 ± 0.5 × $10^5$ HOLO-MnSOD $cell^{-1}$[b] |
| Moles per cell | 0.9 ± 0.2 amol $cell^{-1}$ |
| Cell volume | 19.6 ± 0.8 fL[c] |
| Percent of total protein | 1.4% ± 0.2% |

[a]Based on molecular mass of 21.798 kD. [b]Based on hypothetical homodimer with a molecular mass of 43.696 kD. [c]Based on scanning electron micrography.

### Immunolocalization of MnSOD in Plastids

Immunogold labeling measurements suggest that MnSOD is mainly confined to the chloroplast (Fig. 4). The immunogold label is predominantly associated with thylakoid membranes and the pyrenoid. It is not associated with the cytosol or the mitochondria. Because the chloroplast-localized MnSOD is regulated by the nuclear-encoded *sod*A gene, plastid/endoplasmic reticulum transit peptides must be present, but they have not yet been identified.

### Impact of Light on TpMnSOD Expression

When acclimated to a range of irradiance levels (25, 50, 120, 350, and 800 $\mu$mol $m^{-2}$ $s^{-1}$), *T. pseudonana* cells show a 73% increase in growth rate (Fig. 5). Total chlorophyll *a* $cell^{-1}$ is constant at low light levels (25–50 $\mu$mol $m^{-2}$ $s^{-1}$) but decreases by 63% as the incident light intensity increases from 50 to 800 $\mu$mol $m^{-2}$ $s^{-1}$. (Cells were kept optically thin in semicontinuous batch cultures to avoid self shading.) Over this range of irradiances, the amount of TpMnSOD per unit chlorophyll increased by 60% (Fig. 5), reflecting changes in the chlorophyll concentration, not MnSOD. Although the chlorophyll *a*-normalized MnSOD content of *T. pseudonana* increased with increasing light, the amount of MnSOD per total cellular protein was constant (data not shown). Thus, the demand for MnSOD per cell in these cells appears to be constant over these light levels despite declining chlorophyll. A similar relationship between light intensity, SOD, and reduced cellular chlorophyll was also seen for the chloroplastic CuZnSOD in bean and other higher plants (Gonzalez et al., 1998, and refs. therein).

To further examine the relationship between light and MnSOD, the time course of TpMnSOD expression was followed over 30 h in cells acclimated to a 12/12-h photoperiod. TpMnSOD expression did not vary significantly over the photoperiod when grown at 120 $\mu$mol $m^{-2}$ $s^{-1}$ incident light (control), but increased by 40% within 24 h and after one dark period when transferred to high light (>800 $\mu$mol $m^{-2}$ $s^{-1}$; Fig. 6, A and B). The maximum photosynthetic quantum yield ($F_v/F_m$; Kolber et al., 1998) initially decreased by 50% under high light but recovered and exceeded the control within 30 h (Fig. 6, A and B). After a period of recovery (the dark cycle) to reorganize their metabolic profile, the cells then effectively cope with the high light stress with increased MnSOD expression. The increase in MnSOD expression per unit protein in the high light treatment (12/12-h light/dark) is significant ($P = 0.0007$) and is not exhibited by cells exposed to continuous high light. MnSOD expression, normalized to cell protein, doubled after transfer from culture grown in continuous light to a 12/12-h light/dark cycle (data not shown). Thus, continuous light apparently results in greater oxidative stress in diatoms than does a diel light cycle.

## DISCUSSION

Our results clearly indicate that in *T. pseudonana* MnSOD is localized in the chloroplasts. This subcellular location is in contrast with all other cellular MnSOD distributions in eukaryotic photoautotrophs, where MnSOD is found exclusively in the mitochondria (Grace, 1990; Moller, 2001; del Rio et al., 2003). The presence of MnSOD in the chloroplast results in cells having a high cellular Mn requirement, given the substantial need for Mn of the photosynthetic machinery. The localization of this nuclear-encoded gene in a secondary symbiont presumably facilitates the rapid destruction of SOD, which is inevitably photochemically generated from the reaction centers in both photosystems. For example, the D1 protein (PsbA) has a turnover rate of approximately 30 min, one of the fastest turnover protein rates on Earth (Kim et al., 1993; Sundby et al., 1993; Andersson and Aro, 1997; Neidhardt et al., 1998). This high turnover is due, in large part, to the production of radical oxygen on the donor side of PSII (Mattoo et al., 1984). Chloroplast

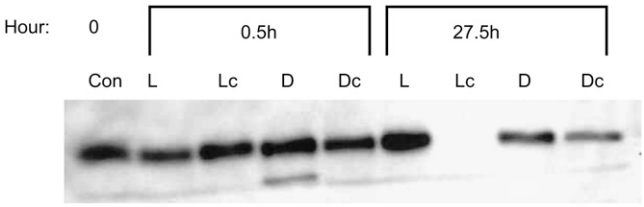


**Figure 2.** Immunoblot of *T. pseudonana* CCMP1335 cells and cells treated with 10 mg/mL cycloheximide (L = light, D = dark, Lc = light + cycloheximide, Dc = dark + cycloheximide) to inhibit protein synthesis. After 27 h, the protein is below detection in the cells grown under light with protein synthesis inhibited. This suggests that the turnover of TpMnSOD is related to processes that occur when cells are exposed to light. Conversely, cells exposed to continuous darkness show evidence of TpMnSOD throughout the experiment. Each lane is loaded with 8 $\mu$g of total protein extracts. Antibody was specifically raised against recombinant protein in control lane.

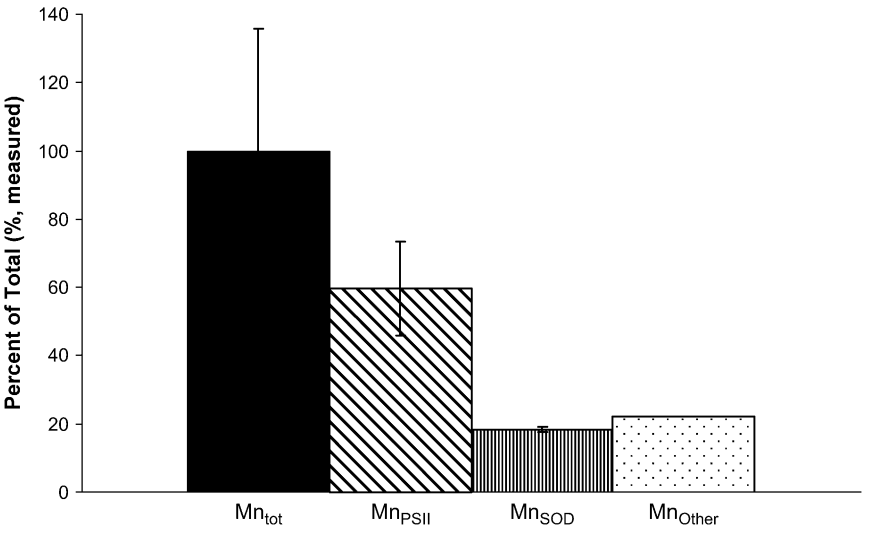


**Figure 3.** Intracellular distribution of Mn for *T. pseudonana* CCMP1335. Total cellular Mn ($Mn_{tot}$) was estimated from the $C_{org}$-specific Mn quotas (micromoles Mn per moles C) of Sunda and Huntsman (1998; Fig. 7; Table II) and the $C_{org}$ content of mid-log exponentially growing cells (0.89 pmol $C_{org}$ $cell^{-1}$). Mn in PSII ($Mn_{PSII}$) is that modeled by Raven (1990). Mn in SOD was estimated as the average measured MnSOD concentration using the quantitative immunotechnique (moles of MnSOD per cell; Table II). Note that as $C_{org}$ decreases in cells as light increases while moles of MnSOD per cell stays constant across light levels, the percent of Mn in MnSOD may increase with irradiance (see also Fig. 5). Error indicated is SE (values are means, $n = 2 \pm$ SE).

specific SODs influence the D1 protein turnover due to their role in catalyzing the destruction of ROS in the chloroplast (Barber and Andersson, 1992; Aro et al., 1993; Andersson and Aro, 1997). If diatoms use MnSOD to suppress oxidative stress associated with photosynthesis in the chloroplast, we would expect diatoms to have higher Mn requirements than other classes of phytoplankton. Indeed, the measured cellular Mn quota of diatoms is significantly higher than that reported for other eukaryotic algae (Raven, 1990; Raven et al., 1999; Ho et al., 2003; Quigg et al., 2003).

Given the potentially large Mn requirement associated with photosynthesis, a great deal of effort has been focused on determining the cellular Mn budget in marine phytoplankton. Current cellular Mn budget estimates for diatoms have been based solely on the Mn associated with PSII (Raven, 1990). These budgets significantly underestimate measured cellular Mn concentrations (Sunda and Huntsman, 1986, 1998; Peers and Price, 2004); however, including MnSOD (10%–20% of total cellular Mn), up to 80% of the total cellular Mn can be accounted for, all of which is in the chloroplasts (Sunda and Huntsman, 1986, 1998; Raven, 1990; Peers and Price, 2004).

Mn does not appear to be biolimiting in the oceans. Concentration profiles from numerous ocean basins show that Mn is often at biologically accessible concentrations, while Fe is typically undetectable in surface waters (Li, 1991; Shiller, 1997; Nozaki et al., 1998; Whitfield, 2001). Measured values for Mn in the Atlantic basin range from about 25 nmol $kg^{-1}$ in coastal regions to between 2 and 5 nmol $kg^{-1}$ at open ocean stations (Shiller, 1997). Using average values of chlorophyll as a proxy for biomass (5 $\mu$g $kg^{-1}$ and 1 $\mu$g $kg^{-1}$ for coastal and oceanic regions, respectively [Falkowski and Raven, 1997] and an average of 77 $\mu$g MnSOD mg chlorophyll $a^{-1}$ [based on our measurements; see Fig. 5]), we calculated that oceanic Mn concentrations support more than 1,000 turnovers of Mn in diatoms assuming growth rate between 1 and 2 $d^{-1}$. Mn could thus serve as a possible metal replacement for Fe and other biolimiting metals in marine algae (Whitfield, 2001; Peers and Price, 2004).

The high Mn requirement of diatoms is significant to the ecology of these eukaryotic algae, as the role of trace metals has been shown to structure oceanic phytoplankton productivity and community composition in many regions (Saito et al., 2003; Coale et al., 2004). A major focus of research has been on Fe, which limits productivity and is only present in subnanomolar concentrations in most of the world's oceans (Boyd et al., 2000; Coale et al., 2004). Therefore, it is not surprising that some photoautotrophs have evolved mechanisms to compensate for low Fe availability. For example, diatoms can use flavodoxin, instead of the Fe-requiring ferredoxin, under low Fe conditions to support electron transport in PSI (LaRoche et al., 1993; McKay et al., 1999). Similarly, some cyanobacteria and chlorophytes substitute the Cu-containing plastocyanin for the Fe-heme cytochrome $c_6$ in PSI to transfer electrons between the cytochrome $b_6f$ complex and $P700^+$ (Quinn and Merchant, 1999). This strategy appears to have been selected on substituting a limiting metal in a pathway with a more available and accessible metal in the same biochemical role.

This strategic biochemical substitution suggests that phytoplankton living in chronically Fe-limited waters may gain a competitive advantage if they can use alternative metals. Cyanobacteria from oligotrophic areas contain either NiSOD alone or both Ni and MnSOD instead of FeSOD found in freshwater species (Partensky et al., 1999; Palenik et al., 2003; Wolfe-Simon et al., 2005). Thus, two of the most successful groups of marine phytoplankton (diatoms and cyanobacteria; Falkowski et al., 2004a, 2004b) use non-Fe SODs to cope with oxidative stress in the Fe-poor regions of the modern ocean. Modern chlorophytes, including embryophytes, do not use Fe enzyme replacements. Therefore, it is not surprising that these taxa are not

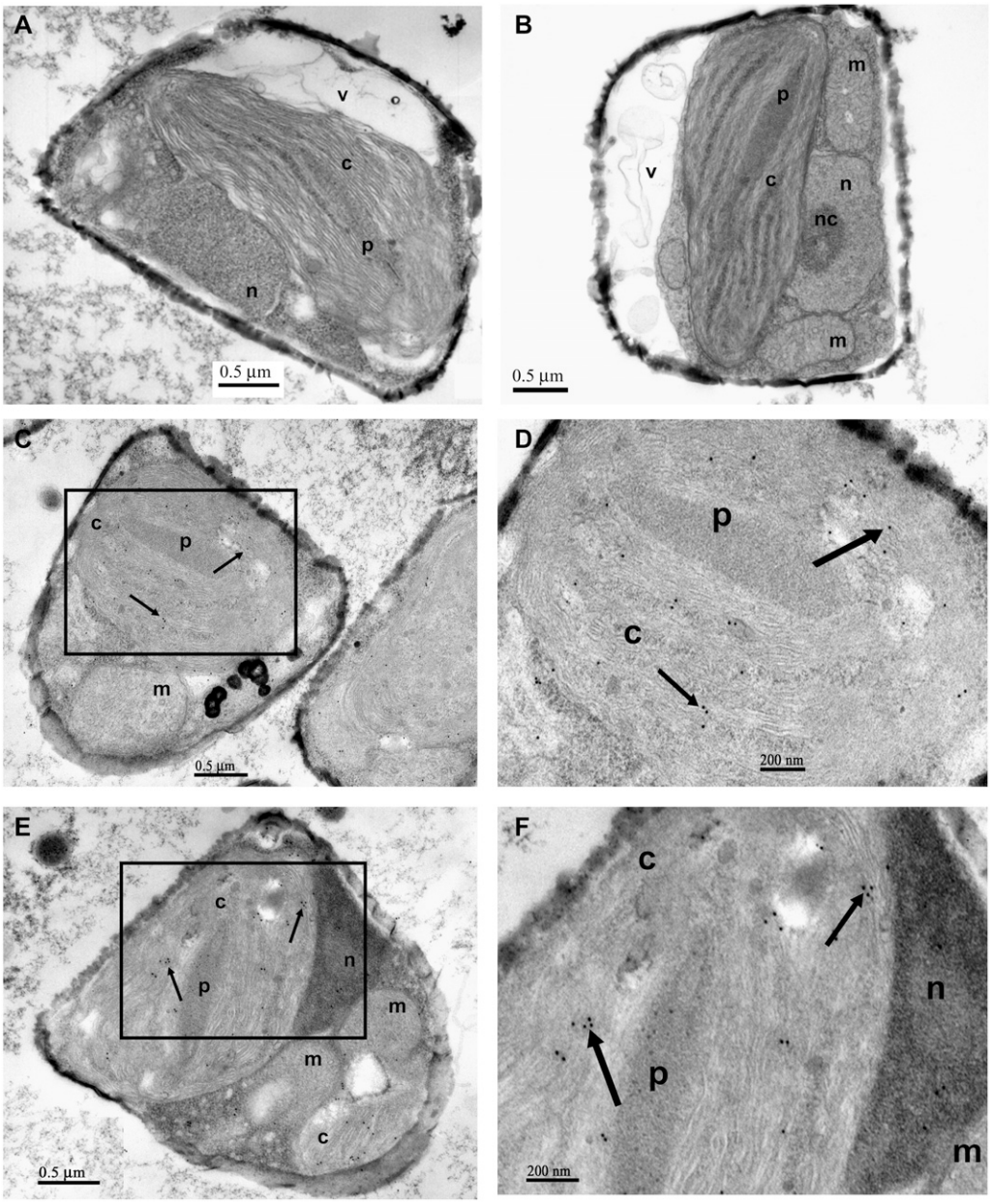


**Figure 4.** Immunogold localization of MnSOD in *T. pseudonana* CCMP1335. A, Osmium tetroxide-stained electron micrograph of whole cell. B, A second different view of osmium tetroxide-stained cell. C, Immunogold labeling of the chloroplast with the anti-TpMnSOD antibody. D, Magnified view of delineated area in B. E, Immunogold labeling of the chloroplast in another cell of *T. pseudonana*. F, Magnified view of delineated area in E. Note the absence of labeling of mitochondrial and cytosolic regions. c, Chloroplast; p, pyrenoid; m, mitochondrion; n, nucleus; nc, nucleolus; v, vacuole. Arrows indicate black, electron-dense gold label corresponding to TpMnSOD. Faint and less electron-dense granules also apparent in the pyrenoid are crystalline formations of almost pure Rubisco (Falkowski and Raven, 2007). Scale bars are length as indicated.

dominant in the oceans and are found primarily in terrestrial, freshwater, and estuarine systems that have abundant Fe concentrations (Sterner et al., 2004). Thus, utilization of MnSODs may be one more mechanism underlying the dominance of red alga taxa over the last 275 million years (Falkowski et al., 2004a, 2004b).

The ancient aquatic ecosystem is thought to have been chemically reduced, which would have made Fe abundantly available to evolving organisms (Canfield, 1998; Brocks et al., 1999; Anbar and Knoll, 2002). As oxygen increased and oxidized most of the Fe to an insoluble oxide form, organisms were forced to evolve alternative options for biochemical pathways. Fe is still biochemically utilized for many electron transfer reactions. However, at protein active sites where Mn could substitute for Fe with few genetic mutations, Mn was often appropriated. This is especially true for electron transfer reactions involving $O_2$.

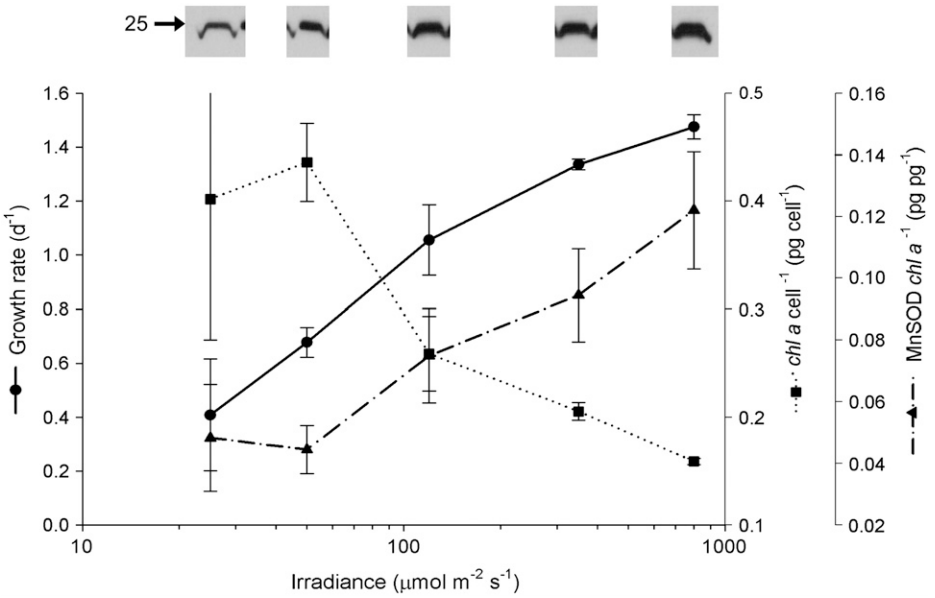


**Figure 5.** Comparison of growth rate, total cellular chlorophyll, and MnSOD per unit chlorophyll of *T. pseudonana* CCMP1335 cells grown at different continuous light intensities. Immunoblot images above the graph are of protein samples loaded according to equal chlorophyll concentrations. Growth rate (black circles and solid line) increases by 2-fold over these light levels. Concurrently, cellular chlorophyll (black squares, dotted line) decreases. Although MnSOD is constant per unit protein (data not shown), MnSOD per unit chlorophyll (black triangles, dashed and dotted line; western blot above image) increases. This supports the strong association of the relative contribution of MnSOD in the chloroplast to protecting the photosynthetic machinery, especially as the light-harvesting pigments decrease. Values are means, $n = 2 \pm$ SD.

Chlorophytes (as well as some embryophytes) typically utilize FeSOD isoforms in the chloroplast (Sakurai et al., 1993; Chen et al., 1996; Kitayama et al., 1999). Consequently, the use of MnSOD in the chloroplast should lower a cell's Fe demand because there is less FeSOD in use. These proteomic differences are reflected in the metal quotas of various marine phytoplankton taxa as diatoms have significantly lower Fe requirements than chlorophytes (Ho et al., 2003; Quigg et al., 2003). Furthermore, this biochemical difference may reflect the environments under which the diverse photosynthetic taxa evolved (Williams, 1981). Thus, the nutritional difference of Mn between chlorophytes and diatoms may contribute to the success of the diatoms in the low Fe modern marine environment (Falkowski et al., 2004a).

## MATERIALS AND METHODS

### Organisms, Culture Conditions, and Standard Protocols

Axenic cultures of *Thalassiosira pseudonana* CCMP1335 cells were used for all manipulations, including nucleic acid isolation and physiological studies. Cells were maintained in F/2+Si medium (Guillard and Ryther, 1962; Guillard, 1975) at a salinity of 35 practical salinity units and 20°C with aeration under fluorescent cool-white lamps with an incident light intensity of 120 $\mu$mol m$^{-2}$ s$^{-1}$ unless otherwise stated. Chlorophyll *a* was analyzed using standard 90% acetone extractions from glass fiber filtered culture (Jeffrey and Humphrey, 1975) measured on a spectrophotometer (Agilent 8453E; Agilent Technologies). Variable fluorescence ($F_v/F_m$) was acquired using a fast repetition rate fluorometer (Kolber et al., 1998). Total carbon (inorganic and organic, subset of samples acidified to remove inorganic carbon) and nitrogen content of cultures were measured with a Carlo Erba NA-1500 elemental analyzer.

### Cloning and Purification of Recombinant TpMnSOD

Total nucleic acids from mid-log growth *T. pseudonana* cells were extracted and treated with DNA-free (catalog no. 1906; Ambion) to remove DNA. First-strand cDNA was synthesized with total RNA using M-MLV Reverse Transcriptase (catalog no. 28025–013; Invitrogen). The cDNA was then used as a template for PCR to amplify *sod*A with the specific primers 5′-ATGAAAATCCATCATGATAAGCAT-3′ and 5′-TCCTCGCACGGGGACTCCTG-3′. The full copy of the gene was then cloned into the pBAD vector (catalog no. K4300–40; Invitrogen) and transformed into *Escherichia coli* for overexpression. The expression of the protein was controlled by varying the concentration of Ara to achieve ideal expressed product. The vector contains a poly His-tag as well as a V5 epitope region. Thus, the recombinant protein was purified using Ni-NTA resin (catalog nos. 30230 and 30410; Qiagen) using both gravity chromatography and FPLC.

### Antibody Production against TpMnSOD

For the initial immunization, equal volumes of recombinant TpMnSOD protein in a 2 mg/mL concentration and Freund's Complete adjuvant were emulsified using a micro-emulsifying needle. A total of 0.8 mL of the emulsified protein and adjuvant were injected subcutaneously into two New Zealand White rabbits in four sites (maximum 0.2 mL/site). A subsequent injection was given 30 d later and was prepared using equal volumes of the provided antigen in a 1 mg/mL concentration and Freund's Incomplete adjuvant. The emulsified protein and adjuvant were injected subcutaneously with a maximum of 0.2 mL/site. Subsequent injections were given at 30- to 35-d intervals. Blood draws from the central ear artery were performed between 10 and 20 d after each subsequent injection. The maximum blood withdrawn did not exceed the standard recommendation of blood amount withdrawn of 15% of total blood volume, or 1% of body weight.

### Immunoblot Analyses

Protein was extracted from cell pellets in 2% SDS, 0.05 M sodium carbonate, 7.5% glycerol, 0.025% bromothymol blue, 5 mm phenylmethylsulfonyl fluoride, and 0.1 M dithiothreitol. Sample protein concentration was quantified using either the bicinchoninic acid method (catalog no. 23227; Pierce Biotechnology) or a fluorescent method (catalog no. R33200; Invitrogen). Samples were then run on 12%, 15%, or 18% (w/v) polyacrylamide gels and then blotted onto polyvinylidene fluoride membrane (Towbin et al., 1979). The blots were then probed with anti-TpMnSOD, the antibody raised against the recombinant MnSOD in *T. pseudonana*. A horseradish peroxidase-conjugated secondary antibody (catalog no. 172–1019; Bio-Rad Laboratories) was used according to instructions and the blots were visualized with a chemiluminescent substrate system on film (catalog no. 34080; Pierce Biotechnology). For quantitative immunoblot, known concentrations of both cells (total no.) and protein (total micrograms) were run on three separate gels and then compared to unknown samples using densitometry.

### Immunogold Staining

After fixation for 3 h in a modified electron microscopy fixative (3% sodium chloride, 0.1 M sodium cacodylate, 2.5% glutaraldehyde, pH 7.4), cell pellets were rinsed three times in Eppendorf tubes (2 × 15 min and 1 × overnight) in 3% sodium chloride, 0.1 M sodium cacodylate, pH 7.4 (cells for transmission

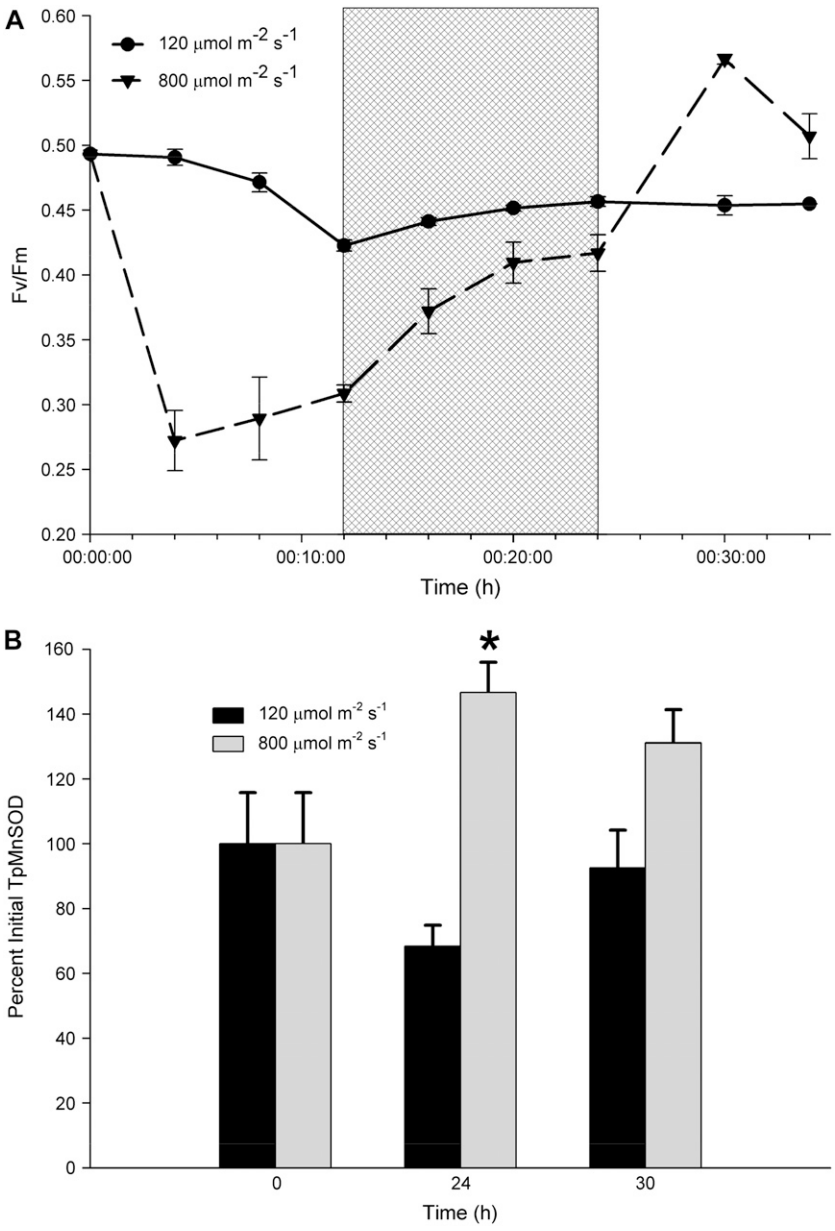


**Figure 6.** Diel expression of MnSOD in *T. pseudonana* CCMP1335. A, This figure demonstrates the quantum yield ($F_v/F_m$) of cells exposed to 12/12-h light/dark cycle under high light (800 $\mu$mol $m^{-2}$ $s^{-1}$, black triangles and dashed line) and control light (120 $\mu$mol $m^{-2}$ $s^{-1}$, black circles and solid line) over time (*x* axis). $F_v/F_m$ decreases in the high light over the first 12 h when compared to the control and then recovered during and after the dark period. The dark period is represented by the shaded area. B, Immunoblot densitometric analysis shows significant recovery after the dark period of TpMnSOD in the high light (hatched bars) treatment as compared to the expression of TpMnSOD in the control light (solid bars) cultures (values are means, $n = 2 \pm$SD). *, Significant differences between treatments ($P = 0.0105$).

electron microscopy imaging only were also postfixed for 2 h in 1% buffered osmium tetroxide). After the washes, the cells were then dehydrated through a graded series of ethanol washes, starting with 50% ethanol to 100% ethanol. The pellets were then embedded in Dr. Spurr's Low Viscosity Embedding Media within the Eppendorf tubes.

Sections were cut using a LKB 2088 ultramicrotome (LKB-Produkter, S–161 25) collected on 300-mesh gold grids and immunostained. Briefly, each grid was incubated for 1 h in Tris-buffered saline plus Tween 20 (TBST; 0.02 M Tris, 0.15 M NaCl, 0.1% Tween 20) + 0.5% bovine serum albumin, pH 7.6. The grids were then transferred to primary antibody diluted in TBST (50-$\mu$L drops). The grids were then incubated overnight in a humidified chamber at 4°C. The next morning, the grids and solutions were left to come to room temperature and the grids were washed 10 times, 1 min each time. Then the grids were transferred to the appropriate gold-labeled secondary antibody (1:20 or 1:15; catalog no. G7402; Sigma-Aldrich) diluted in TBST. They were incubated in the secondary antibody for 1 h at room temperature. Control grids were stained only with the secondary gold-labeled antibody. The grids were washed 10 times, 1 min each in TBST, then the same amount of times in ultrapure water. The grids were then counter-stained with uranyl acetate and lead citrate and photographed in a JEM-100CXII electron microscope (JEOL) at 80 kV.

## ACKNOWLEDGMENTS

We thank Charlotte Fuller, Alois Trey, Alicia Jones, Daniel Grzebyk, Kathleen McGuirk, and Jonathan Simon for helpful laboratory assistance. Also, we express our appreciation to Lin Jiang and Dov Chelst for aid with statistical analyses, Bill Sunda for thoughtful discussions, and three anonymous reviewers for helpful comments that improved the quality of this manuscript.

Received September 1, 2006; accepted October 16, 2006; published October 20, 2006.

## LITERATURE CITED

**Anbar AD, Knoll AH** (2002) Proterozoic ocean chemistry and evolution: a bioinorganic bridge? Science **297:** 1137–1142

**Anderson JM, Park Y-I, Chow WS** (1999) Unifying model for the photoinactivation of Photosystem II *in vivo* under steady-state photosynthesis. Photosynth Res **56:** 1–13

**Andersson B, Aro EM** (1997) Proteolytic activities and proteases of plant chloroplasts. Physiol Plant **100:** 780–793

**Apel K, Hirt H** (2004) Reactive oxygen species: metabolism, oxidative stress, and signal transduction. Annu Rev Plant Biol **55:** 373–399

**Aro EM, Virgin I, Andersson B** (1993) Photoinhibition of Photosystem II. Inactivation, protein damage and turnover. Biochim Biophys Acta **1143:** 113–134

**Asada K** (1999) The water-water cycle as alternative photon and electron sinks. Philos Trans R Soc Lond B Biol Sci **355:** 1419–1431

**Barber J, Andersson B** (1992) Too much of a good thing: light can be bad for photosynthesis. Trends Biochem Sci **17:** 61–66

**Bowler C, Montagu MV, Inze D** (1992) Superoxide dismutase and stress tolerance. Annu Rev Plant Physiol Plant Mol Biol **43:** 83–116

**Boyd PW, Watson AJ, Law CS, Abraham ER, Trull T, Murdoch R, Bakker DC, Bowie AR, Buesseler KO, Chang H, et al** (2000) A mesoscale phytoplankton bloom in the polar Southern Ocean stimulated by iron fertilization. Nature **407:** 695–702

**Brocks JJ, Logan GA, Buick R, Summons RE** (1999) Archean molecular fossils and the early rise of eukaryotes. Science **285:** 1033–1036

**Cabecadas L, Brogueira MJ, Cabecadas G** (1999) Phytoplankton spring bloom in the Targus coastal waters: hydrological and chemical conditions. Aquat Ecol **33:** 243–250

**Canfield DE** (1998) A new model for Proterozoic ocean chemistry. Nature **396:** 450–453

**Chen H, Romo-Leroux PA, Salin ML** (1996) The iron-containing superoxide dismutase-encoding gene from *Chlamydomonas reinhardtii* obtained by direct and inverse PCR. Gene **168:** 113–116

**Chen J, Liao C, Mao SJ, Chen T, Weng C** (2001) A simple technique for the simultaneous determination of molecular weight and activity of superoxide dismutase using SDS-PAGE. J Biochem Biophys Methods **47:** 233–237

**Coale KH, Johnson KS, Chavez FP, Buesseler KO, Barber RT, Brzezinski MA, Cochlan WP, Millero FJ, Falkowski PG, Bauer JE, et al** (2004) Southern Ocean iron enrichment experiment: carbon cycling in high- and low-Si waters. Science **304:** 408–414

**del Rio LA, Sandalio LM, Altomare DA, Zilinskas BA** (2003) Mitochondrial and peroxisomal manganese superoxide dismutase: differential expression during leaf senescence. J Exp Bot **54:** 923–933

**Falkowski P, Raven J** (2007) Aquatic Photosynthesis, Ed 2. Princeton University Press, Princeton

**Falkowski PG, Katz ME, Knoll AH, Quigg A, Raven JA, Schofield O, Taylor FJR** (2004a) The evolution of modern eukaryotic phytoplankton. Science **305:** 354–360

**Falkowski PG, Raven JA** (1997) Aquatic Photosynthesis. Blackwell Science, Malden, MA

**Falkowski PG, Schofield O, Katz ME, Schootbrugge BVD, Knoll A** (2004b) Why is the land green and the ocean red? *In* H Thierstein, J Young, eds, Coccolithophorids. Springer-Verlag, Berlin

**Fink RC, Scandalios JG** (2002) Molecular evolution and structure-function relationships of the superoxide dismutase gene families in angiosperms and their relationship to other eukaryotic and prokaryotic superoxide dismutases. Arch Biochem Biophys **399:** 19–36

**Fridovich I** (1995) Superoxide radical and superoxide dismutase. Annu Rev Biochem **64:** 97–112

**Gonzalez A, Steffen KL, Lynch JP** (1998) Light and excess manganese. Plant Physiol **118:** 493–504

**Grace SC** (1990) Phylogenetic distribution of superoxide dismutase supports an endosymbiotic origin for chloroplasts and mitochondria. Life Sci **47:** 1875–1886

**Guillard RRL** (1975) Culture of phytoplankton for feeding marine invertebrates. *In* WL Smith, MH Chanley, eds, Culture of Marine Invertebrate Animals. Plenum Press, New York, pp 29–60

**Guillard RRL, Ryther JH** (1962) Studies of marine planktonic diatoms. I. *Cyclotella nana* Hustedt and *Detonula confervacea* Cleve. Can J Microbiol **8:** 229–239

**Halliwell B** (1982) The toxic effects of oxygen on plant tissues. *In* LW Oberley, ed, Superoxide Dismutase, Vol I. CRC Press, Boca Raton, FL, pp 89–124

**Herbert SK, Samson G, Fork DC, Laudenbach DE** (1992) Characterization of damage to photosystems I and II in a cyanobacterium lacking detectable iron superoxide dismutase activity. Proc Natl Acad Sci USA **89:** 8716–8720

**Ho T-Y, Quigg A, Finkel ZV, Mulligan A, Wyman K, Falkowski PG, Morel FMM** (2003) On the elemental composition of some marine phytoplankton. J Phycol **39:** 1145–1159

**Huang JK, Wen L, Ma H, Huang ZX, Lin CT** (2005) Biochemical characterization of a cambialistic superoxide dismutase isozyme from diatom *Thallassiosira weissflogii*: cloning, expression, and enzyme stability. J Agric Food Chem **53:** 6319–6325

**Jeffrey SW, Humphrey GF** (1975) New spectrophotometric equations for determining chlorophylls a, b, c1 and c2 in higher plants, algae, and natural phytoplankton. Biochem Physiol Pflanz **167:** 191–194

**Ken CF, Hsiung TM, Huang ZX, Juang RH, Lin CT** (2005) Characterization of Fe/Mn-superoxide dismutase from diatom *Thallassiosira weissfloii*: cloning, expression, and property. J Agric Food Chem **53:** 1470–1474

**Kim JH, Nemson JA, Melis A** (1993) Photosystem II reaction center damage and repair in *Dunaliella salina* (green alga): analysis under physiological and irradiance-stress conditions. Plant Physiol **103:** 181–189

**Kitayama K, Kitayama M, Osafune T, Togasaki RK** (1999) Subcellular localization of iron and manganese superoxide dismutase in *Chlamydomonas reinhardtii* (Chlorophyceae). J Phycol **35:** 136–142

**Kliebenstein DJ, Monde RA, Last RL** (1998) Superoxide dismutase in Arabidopsis: an eclectic enzyme family with disparate regulation and protein localization. Plant Physiol **118:** 637–650

**Kolber ZS, Prasil O, Falkowski PG** (1998) Measurement of variable chlorophyll fluorescence using fast repetition rate techniques: defining methodology and experimental protocols. Biochim Biophys Acta **1367:** 88–106

**LaRoche J, Geider RJ, Graziano LM, Murray H, Lewis K** (1993) Induction of specific proteins in eukaryotic algae grown under iron-, phosphorus-, or nitrogen-deficient conditions. J Phycol **29:** 767–777

**Levasseur M, Fortier L, Therriault J-C, Harrison PJ** (1992) Phytoplankton dynamics in a coastal jet frontal region. Mar Ecol Prog Ser **86:** 283–295

**Li T, Huang X, Zhou R, Liu Y, Li B, Nomura C, Zhao J** (2002) Differential expression and localization of Mn and Fe superoxide dismutases in the heterocystous cyanobacterium *Anabaena* sp. strain PCC 7120. J Bacteriol **184:** 5096–5103

**Li Y-H** (1991) Distribution patterns of the elements in the ocean: a synthesis. Geochim Cosmochim Acta **55:** 3223–3240

**Mattoo AK, Hoffman-Falk H, Marder JB, Edelman M** (1984) Regulation of protein metabolism: coupling of photosynthetic electron transport to in vivo degradation of the rapidly metabolized 32-kilodalton protein of the chloroplast membranes. Proc Natl Acad Sci USA **81:** 1380–1384

**McKay RM, Roche JL, Yakunin AF, Durnford DG, Geider RJ** (1999) Accumulation of ferredoxin and flavodoxin in a marine diatom in response to Fe. J Phycol **35:** 510–519

**Moller IM** (2001) Plant mitochondria and oxidative stress: electron transport, NADPH turnover, and metabolism of reactive oxygen species. Annu Rev Plant Physiol Plant Mol Biol **52:** 561–591

**Neidhardt J, Benemann JR, Zhang L, Melis A** (1998) Photosystem-II repair and chloroplast recovery from irradiance stress: relationship between chronic photoinhibition, light-harvesting chlorophyll antenna size and photosynthetic productivity in *Dunaliella salina* (green algae). Photosynth Res **56:** 175–184

**Nozaki Y, Yamada M, Nakanishi T, Nagaya Y, Nakamura K, Shitashima K, Tsubota H** (1998) The distribution of radionuclides and some trace metals in the water columns of the Japan and Bonin trenches. Oceanol Acta **21:** 469–484

**Okamoto OK, Robertson DL, Fagan TF, Hastings JW, Colepicolo P** (2001) Different regulatory mechanisms modulate the expression of a dinoflagellate iron-superoxide dismutase. J Biol Chem **276:** 19989–19993

**Okomoto OK, Pinto E, Latorre LR, Bechara EJH, Colepicolo P** (2001) Antioxidant modulation in response to metal-induced oxidative stress in algal chloroplasts. Arch Environ Contam Toxicol **40:** 18–24

**Palenik B, Brahamsha B, Larimer FW, Land M, Hauser L, Chain P, Lamerdin J, Regala W, Allen EE, McCarren J, et al** (2003) The genome of a motile marine *Synechococcus*. Nature **424:** 1037–1042

**Partensky F, Hess WR, Vaulot D** (1999) *Prochlorococcus*, a marine photosynthetic prokaryote of global significance. Microbiol Mol Biol Rev **63:** 106–127

**Peers G, Price NM** (2004) A role for manganese in superoxide dismutases and growth of iron-deficient diatoms. Limnol Oceanogr **49:** 1774–1783

**Quigg A, Finkel ZV, Irwin AJ, Reinfelder JR, Rosenthal Y, Ho T-Y, Schofield O, Rosenthal FMM, Falkowski PG** (2003) The evolutionary inheritance of elemental stoichiometry in marine phytoplankton. Nature **425:** 291–294

**Quinn JM, Merchant S** (1999) Adaptation of *Senedesmus obliquus* (Chlorophyceae) to copper-deficiency: transcriptional regulation of *Pcy1* but not *Cpx1*. J Phycol **35:** 1253–1263

**Raven JA** (1990) Predictions of Mn and Fe use efficiencies of phototrophic growth as a function of light availability for growth and of C assimilation pathway. New Phytol **116:** 1–18

**Raven JA, Evans MCW, Korb RE** (1999) The role of trace metals in photosynthetic electron transport in $O_2$-evolving organisms. Photosynth Res **60:** 111–149

**Raychaudhuri SS, Deng XW** (2000) The role of superoxide dismutase in combating oxidative stress in higher plants. Bot Rev **66:** 89–98

**Saito MA, Sigman DM, Morel FMM** (2003) The bioinorganic chemistry of the ancient ocean: the co-evolution of cyanobacterial metal requirements and biogeochemical cycles at the Archean-Proterozoic boundary? Inorg Chim Acta **356:** 308–318

**Sakurai H, Kususmoto N, Kitayama K, Togasaki RK** (1993) Isozymes of superoxide dismutase in *Chlamydomonas* and purification of one of the major isozymes containing Fe. Plant Cell Physiol **34:** 1133–1137

**Scandalios JG** (1993) Oxygen stress and superoxide dismutases. Plant Physiol **101:** 7–12

**Shiller AM** (1997) Manganese in surface waters of the Atlantic Ocean. Geophys Res Lett **24:** 1495–1498

**Sterner RW, Smutka TM, McKay RML, Xiaoming Q, Brown ET, Sherrell RM** (2004) Phosphorus and trace metal limitation of algae and bacteria in Lake Superior. Limnol Oceanogr **49:** 495–507

**Sunda WG, Huntsman SA** (1986) Relationships among growth rate, cellular manganese concentrations and manganese transport kinetics in estuarine and oceanic species of the diatom *Thalassiosira*. J Phycol **22:** 259–270

**Sunda WG, Huntsman SA** (1998) Interactive effects of external manganese, the toxic metals copper and zinc, and light in controlling cellular manganese and growth in a coastal diatom. Limnol Oceanogr **43:** 1467–1475

**Sundby C, McCaffery S, Anderson JM** (1993) Turnover of the photosystem II D1 protein in higher plants under photoinhibitory and nonphotoinhibitory irradiance. J Biol Chem **268:** 25476–25482

**Towbin H, Staehelin T, Gordon J** (1979) Electrophoretic transfer of proteins from polyacrylamide gels to nitrocellulose sheets: procedure and some applications. Proc Natl Acad Sci USA **76:** 4350–4354

**Whitfield M** (2001) Interactions between phytoplankton and trace metals in the ocean. Adv Mar Biol **41:** 1–128

**Williams RJP** (1981) The Bakerian Lecture, 1981: natural selection of the chemical elements. Proc R Soc Lond B Biol Sci **213:** 361–397

**Wolfe-Simon F, Grzebyk D, Schofield O, Falkowski PG** (2005) The role and evolution of superoxide dismutases in algae. J Phycol **41:** 453–465

**Wu G, Wilen RW, Robertson AJ, Gusta LV** (1999) Isolation, chromosomal localization, and differential expression of mitochondrial manganese superoxide dismutase and chloroplastic copper/zinc superoxide dismutase genes in wheat. Plant Physiol **120:** 513–520

**Zelko IN, Manriani YJ, Folz RJ** (2002) Superoxide dismutase multigene family: a comparison of the CuZn-SOD (SOD1), Mn-SOD (SOD2), and EC-SOD (SOD3) gene structures, evolution, and expression. Free Radic Biol Med **33:** 337–349

**Ziemann DA, Conquest LD, Olaizola M, Bienfang PK** (1991) Interannual variability in the spring phytoplankton bloom in Auke Bay, Alaska. Mar Biol **109:** 321–334

**Zigone AR, Casotti R, d'Alcala MR, Scardi M, Marino D** (1995) 'St Martin's Summer': the case of an autumn phytoplankton bloom in the Gulf of Naples (Mediterranean Sea). J Plankton Res **17:** 575–593